

Monoclinic and Triclinic δ -Clathrates of Syndiotactic Polystyrene

Oreste Tarallo* and Vittorio Petraccone

Dipartimento di Chimica "Paolo Corradini", Università degli Studi di Napoli Federico II, Complesso di Monte S. Angelo, via Cintia, 80126 Napoli, Italy

Alexandra R. Albulia, Christophe Daniel, and Gaetano Guerra

Dipartimento di Chimica, INSTM, and NANOMATES Research Unit, Università degli Studi di Salerno, via Ponte Don Melillo, 84084 Fisciano (SA), Italy

Received June 18, 2010; Revised Manuscript Received September 2, 2010

ABSTRACT: The paper compares X-ray diffraction patterns of δ -clathrates of s-PS with a large number of guests, having molecular volume in the range 0.058–0.195 nm³, mainly focusing on the distance between the *ac* layers of enantiomorphous polymer helices (d_{010}), as precisely evaluated by measurements on films exhibiting the $a_{||}c_{||}$ uniplanar orientation. The reported data and the crystal structure determination of the δ -clathrates with dinitrobenzene and dibenzofuran allow concluding that beside the already known large number of δ -clathrates of s-PS with monoclinic unit cells there is also a large number δ -clathrates of s-PS with triclinic unit cells. In particular, monoclinic or triclinic δ -clathrates are generally obtained with guests whose molecular volume is lower or higher with respect to the cavity of the δ nanoporous crystalline form (≈ 0.125 nm³). Small guests are easily accommodated in the cavities of the δ phase, thus maintaining its monoclinic unit cell and $P2_1/a$ symmetry. Bulky guests, on the contrary, can be accommodated by substantial changes of the structural organization of the starting δ nanoporous form, leading to the occupation of only half of the cavities initially present while the other half is lost. This new kind of structural organization of the triclinic δ clathrates allows the inclusion of guest molecules definitely bigger than until now expected, although it halves the maximum guest/styrenic-unit molar ratio, which is reduced from the usual 1/4 to 1/8.

Introduction

Solid polymers with low-molecular-mass active additives find several practical and advanced applications. Several studies have suggested that a simple method to reduce diffusivity of active molecules in the solid state and to prevent their self-aggregation consists of the formation of cocrystals with suitable polymer hosts.¹ This constitutes an innovative approach in the area of functional polymeric materials, which are generally characterized by a disordered distribution of active groups into amorphous phases.

Efficient and versatile appear to be the cocrystalline phases of syndiotactic polystyrene (s-PS), a cheap and robust polymer² with a complex polymorphic behavior, including two crystalline phases (α and β) with trans-planar chains and three crystalline phases (γ , δ , and ϵ) with $s(2/1)2$ helices.³ A particularly relevant feature of s-PS cocrystalline phases is the possibility to achieve three different kinds of uniplanar orientation, which allow to control the orientation of the guest molecules not only in the crystalline phase but also in macroscopic films.⁴ On these bases, films presenting s-PS/active-guest cocrystals have been proposed as advanced materials,⁵ mainly for optical⁵ⁱ (chromophore,^{5b} fluorescent,^{5c,g,h} photoreactive,^{5a,e} non-linear-optical,^{5f} and chiro-optical^{5k}) but also for magnetic^{5d,j} applications.

The control of orientation of guest molecules at macroscopic level, of course, requires a precise knowledge of the structure of the cocrystalline phases. Hence, many studies have been devoted to the definition of the structures of s-PS cocrystalline phases.^{6–8} All the known s-PS cocrystalline phases exhibit as a common

feature the $s(2/1)2$ helical polymer conformation, with a repetition period of nearly 0.78 nm.^{6–8} However, the packing of the host helices and of the guest molecules can largely change, mainly depending on the molecular structure of the guest molecules but also on the preparation procedure.

The large number of s-PS cocrystalline phases can be divided in three classes: intercalates,^{6,9} δ -clathrates⁷ and ϵ -clathrates.⁸ In this respect it is worth adding that, for several guests, cocrystalline phases belonging to two or three of these classes can be obtained. (e.g., δ - and ϵ -clathrates for p-NA and δ -^{7g} and ϵ -clathrates^{8b} as well as intercalate for 2,2,6,6-tetramethylpiperidiny-*N*-oxyl (TEMPO)⁵ⁱ)

Intercalates and δ -clathrate cocrystals described in the literature up to now are all characterized by a common structural feature (which also characterizes the empty δ phase),^{10a} i.e., layers of closely packed enantiomorphous polymer helices (*ac* plane in Figure 1).

For the intercalates, these layers of polymer helices are alternated with layers of guest molecules and the guest/monomer-unit molar ratio is generally 1/2. The spacing between the *ac* layers (d_{010}), for all the known s-PS intercalates is larger than 1.3 nm and values as high as 1.75 nm have been observed.^{6a,b} Intercalate structures have been thoroughly described for the s-PS cocrystals with bicyclo[2,2,1]-hepta-2,5-diene (norbornadiene, NB),^{6a} 1,3,5-trimethylbenzene (TMB),^{6b} and 1,4-dimethylnaphthalene (DMN).^{6b} On the basis of the d_{010} values, the formation of intercalate structures has also been suggested for s-PS cocrystals with 3-carene (3,7,7-trimethylbicyclo[4.1.0]hept-3-ene),^{6b} a styrene dimer (1,4-diphenylbutane),^{9d} TEMPO,⁵ⁱ biphenyl,^{9e} benzophenone,^{9e} diphenylmethane,^{9e} carvone,^{9f} and limonene,^{9f} as well as for s-PS gels in benzene,^{9a} benzyl methacrylate,^{9b} and cyclohexyl methacrylate.^{9c}

*Corresponding author. Telephone: +39-081-674443. Fax: +39-081-674090. E-mail: oreste.tarallo@unina.it.

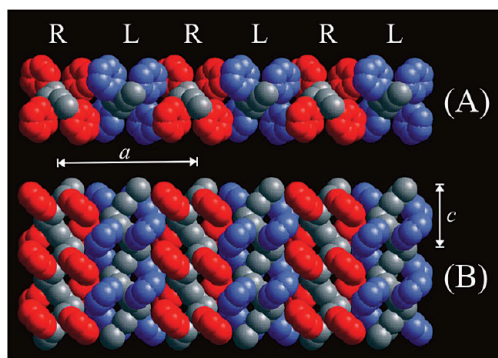


Figure 1. *ac* layers of closely packed enantiomorphous $s(2/1)2$ helices of s-PS, typical of the δ phase as well as of the intercalate and δ -clathrate cocrystalline phases. View along the *c* axis (A) and perpendicular to the *ac* layer (B). R = right-handed and L = left-handed helices.

The δ and ϵ clathrates are cocrystalline phases strictly related to the nanoporous δ^{10} and ϵ^{11} crystalline phases of s-PS. The term of polymeric nanoporous phase (and sometimes the term “polymeric framework”) is used to indicate crystalline polymorphic phases, whose density is lower than the density of the corresponding amorphous phase and being suitable to absorb guest molecules at low activities (e.g., from diluted solutions). Both δ and ϵ phases present a density close to 0.98 g cm^{-3} , i.e., definitely smaller than that one of the amorphous phase (1.05 g cm^{-3}).¹² The packing of the two nanoporous phases is completely different and the empty space is organized as isolated cavities and channels, respectively.

The most relevant structural features of the ϵ -clathrates is that suitable guests are not only small molecules but also long molecules like, e.g., 4-(dimethylamino)cinnamaldehyde which is unable to be enclosed as guest into the isolated cavities of the δ phase.^{11c} Moreover, for the ϵ -clathrates, guest molecules tend to assume orientations with their main molecular axis roughly parallel to the crystalline chain axis.⁸

As for the δ clathrates, the structures described up to now, with the exception of that containing 4-nitroaniline, are similar to that one of the nanoporous δ phase,^{10a} after filling of the isolated cavities with the guest molecules. In particular, all δ clathrates present isolated centrosymmetric guest locations, cooperatively generated by two enantiomorphous helices of two adjacent *ac* polymer layers (Figure 2). Moreover, the efficient packing of the helices in the *ac* plane corresponds to an *a* axis nearly equal for all clathrate cocrystals, independently of the chemical nature of the guest molecule.

For these guest molecules, whose shape and volume are suitable for the isolated cavities of the δ phase, the cocrystalline structures retain the monoclinic $P2_1/a$ symmetry and the cavity shape imposes a guest orientation with their main molecular plane nearly perpendicular to the helical axes. As the bulkiness of the guest increases, there is an increase of the spacing ($d_{010} = b \sin \gamma$) between the *ac* layers (in the range 1.06–1.2 nm).^{6b,7f}

In this respect it is worth noting that this distance (d_{010}) has been suggested as a rapid and efficient criterion to discriminate between δ -clathrate ($d_{010} < 1.2 \text{ nm}$) and intercalate ($d_{010} > 1.3 \text{ nm}$) cocrystalline structures.^{6b}

In a recent paper,^{7g} a different structure has been described for the δ clathrate phase obtained by *p*-nitroaniline (NA) sorption in δ phase samples. In fact, at variance with other known guest molecules (see, e.g., nitrobenzene in Figure 2A) which are accommodated by increasing the interlayer distance (d_{010}) and maintaining their molecular planes perpendicular to the chain axes and the monoclinic symmetry, the NA guest is rather accommodated by shifting along the chain axis the *ac* layers, keeping a d_{010} almost equal to that one of the δ form, thus leading to a unit cell with the α angle not far from 98° (and hence triclinic

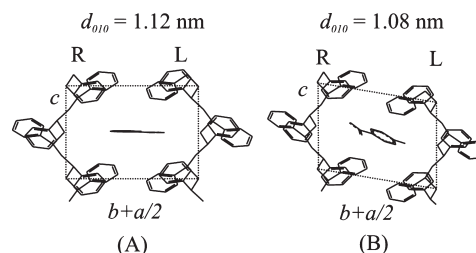


Figure 2. Packing model proposed for the δ -clathrate structures of s-PS with *p*-nitrobenzene (A, monoclinic) and *p*-nitroaniline (B, triclinic).^{7g} Only a couple of enantiomorphous polymer helices (R = right-handed; L = left-handed) that confine the guest molecule is shown. A closer distance between the *ac* layers is observed for the bulkier *p*-nitroaniline guest (B) because the guest is rather accommodated by shifting the *ac* layers along the chain axis, leading to the triclinic symmetry.

rather than monoclinic) and to guest molecular planes inclined with respect to the helical chain axes (Figure 2B).^{7g}

This fact induced us investigating the crystalline structures of several other s-PS clathrate forms, for which, despite the bulkiness of the guest molecules, d_{010} is nearly equal to, or even lower than, that one of the δ form.

Experimental Part

The s-PS used in this study was manufactured by Dow Chemical Company under the trademark Questa 101. The ^{13}C nuclear magnetic resonance characterization showed that the content of syndiotactic triads was over 98%. The weight-average molar mass obtained by gel permeation chromatography (GPC) in trichlorobenzene at 135°C was found to be $M_w = 3.2 \times 10^5$ with the dispersity index $M_w/M_n = 3.9$.

All the solvents and guests molecules used to obtain δ -clathrates were purchased from Aldrich and used without any further purification.

Amorphous films, 150–200 μm thick, were obtained by extrusion of the melt with an extrusion head of 200 mm \times 0.5 mm. Oriented s-PS mesomorphic films were obtained by uniaxial stretching of an amorphous film at 300%, at strain rate of 0.1 s^{-1} , in the temperature range 105–110 $^\circ\text{C}$ with a dynamometer INSTRON 4301.

Oriented nanoporous δ -form films with uniaxial orientation were obtained by immersion in liquid dichloromethane of oriented s-PS mesomorphic films followed by subsequent removal of dichloromethane by immersion in liquid acetonitrile for 24 h. Then, for guest molecules being liquid at room temperature, the δ -clathrate films with uniaxial orientation were obtained by immersion in the pure liquid of the uniaxial δ -form film while for guest molecules being solid at room temperature the δ -clathrate films were obtained by immersion of the uniaxial δ -form film in saturated solutions of acetone for 12 h and subsequent exposure in air until complete acetone removal.

Oriented nanoporous δ -form films exhibiting the uniplanar $a_{||}c_{||}$ orientation were obtained by casting of chloroform solutions followed by subsequent removal of chloroform by immersion in liquid acetonitrile for 24 h. Then, oriented δ -clathrate films with $a_{||}c_{||}$ orientation were obtained applying the same procedure reported above for films with the uniaxial orientation.

X-ray Diffraction. Wide-angle X-ray diffraction patterns of uniplanar $a_{||}c_{||}$ oriented samples were obtained with nickel-filtered Cu K α radiation with an automatic Philips powder diffractometer operating in the $\theta/2\theta$ Bragg–Brentano geometry using 2 mm thick specimen holders.

The X-ray fiber diffraction patterns of oriented samples were obtained under vacuum on a BAS-MS imaging plate (FUJIFILM) with a cylindrical camera (radius 57.3 mm, Ni-filtered Cu K α radiation monochromatized with a graphite crystal) rotating the film around its uniaxial stretching direction. Data were processed with a digital scanner (FUJI-BAS 1800).

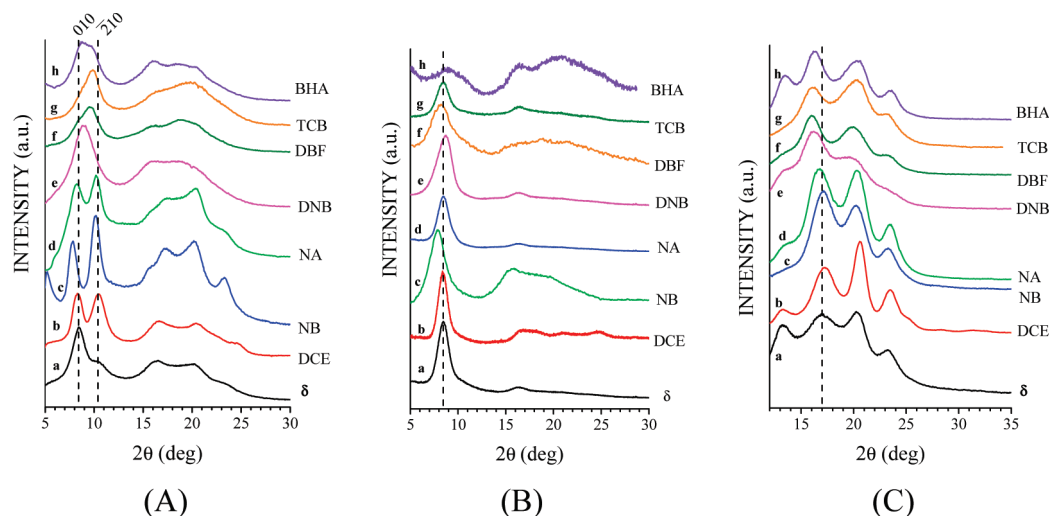


Figure 3. X-ray diffraction patterns of s-PS films exhibiting crystalline or cocrystalline phases: (a) empty δ ; δ -clathrate with (b) dichloroethane (DCE), (c) nitrobenzene (NB), (d) *p*-nitro-aniline (NA), (e) 1,4-dinitro-benzene (DNB), (f) dibenzofuran (DBF), (g) 1,3,5-trichlorobenzene (TCB), and (h) 2-*tert*-butyl-4-methoxyphenol (BHA). (A) Equatorial profiles of fiber-diffraction patterns of uniaxially oriented films. The positions of the 010 and $\bar{2}10$ reflections^{10a} of the nanoporous δ form are indicated with dashed lines. (B) Diffraction patterns of films exhibiting the uniplanar $a_l c_l$ orientation taken in reflection with a powder diffractometer.^{4d} (C) First layer line profiles of fiber-diffraction patterns of the uniaxially oriented films reported in part A.

In order to highlight the position of different reflections, taking into account the conspicuous uniplanar orientation of the cocrystalline films, photographic X-ray fiber diffraction patterns have been also collected by placing the film sample parallel to the axis of the cylindrical camera and by sending the X-ray beam parallel (EDGE) or perpendicular (THROUGH) to the film surface.

Owing to the poor quality of the diffraction patterns, the agreement with the experimental data has been evaluated (Figures 8 and 11) by comparing the experimental X-ray diffraction profiles, read along the equatorial and the first layer lines, after the subtraction of the background and amorphous contributions and the calculated ones according to the structural model proposed.

Calculated intensity profiles were obtained as sum of calculated reflections, each one represented as a Gaussian curve of fixed width, with an area proportional to their calculated intensities and centered at the 2θ calculated according to the unit cell. Only the reflections with intensity stronger than 5% of the most intense one of the whole calculated pattern have been considered. Calculated X-ray reflections have been obtained with the Diffraction-Crystal module of the software package Cerius² (version 4.2 by Accelrys Inc.). To take into account to some extent the disorder described in the text, an isotropic thermal factor B equal to 20 \AA^2 has been used. The used radiation wavelength was 1.5418 \AA (Cu K α). Gaussian profile function having a half-height width regulated by the average crystallite size along a , b , and c axes (L_a , L_b , and L_c , respectively) was used. A good agreement with the experimental profile has been obtained for $L_a = L_b = 10 \text{ nm}$ and $L_c = 8 \text{ nm}$.

Energy Calculation Methods and Volumes. Energy calculations were carried out by using the Compass force field¹³ within the Open Force Field module of Cerius² by the smart minimizer method with standard convergence. The starting conformation of the s-PS polymer chains was that found by molecular mechanics calculations reported in the literature.¹⁴

Volumes of guest molecules have been determined with the Connolly Surface module of Cerius² using a probe radius of 0.11 nm and a density dot of 0.1 nm^{-2} .

Results and Discussion

Distance between ac Layers in δ -Clathrates. This section is devoted to a thorough analysis of the d_{010} distance as observed for different δ -clathrate cocrystalline phases of s-PS with a lot of guest molecules. It is worth pointing out

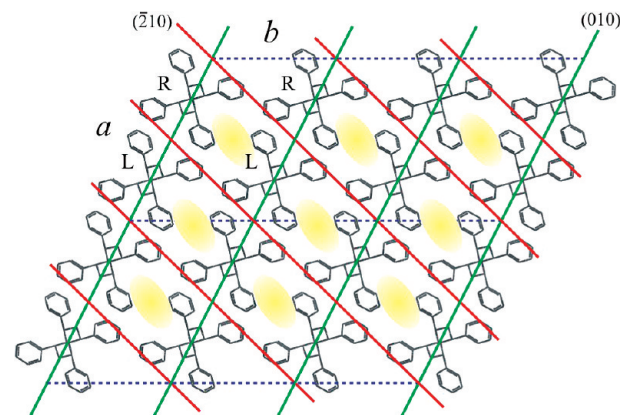


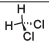
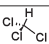
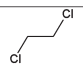
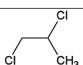
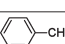
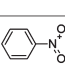
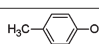
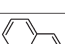
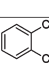
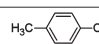
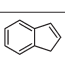
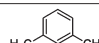
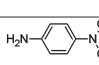
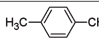
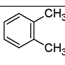
Figure 4. Packing model proposed for the δ form s-PS in the ab projection.^{10a} The (010) and $\bar{2}10$ crystallographic planes have been indicated in green and red, respectively. The nanopores are schematically represented by yellow ellipses. Six unit cells are shown. R = right-handed and L = left-handed helices.

that it is not always possible to obtain the d_{010} value directly from the equatorial layer line of an X-ray fiber diffraction pattern. In this respect, Figure 3A reports the equatorial profiles of the X-ray fiber diffraction patterns of axially oriented s-PS films, exhibiting the nanoporous δ phase, or the cocrystalline phases with a selected number of guest molecules.

As generally observed for δ -clathrates of s-PS, as a consequence of inclusion of guest molecules into the crystalline phase, the diffraction pattern of the δ phase (curve a in Figure 3A) is changed by a reduction of the intensity of the 010 reflection (located for the empty phase at $2\theta_{\text{CuK}\alpha} \approx 8.4^\circ$ corresponding to $d_{010} \approx 1.06 \text{ nm}$) and by an increase of the intensity of the $\bar{2}10$ reflection (located for the empty phase at $2\theta_{\text{CuK}\alpha} \approx 10.6^\circ$ corresponding to $d \approx 0.83 \text{ nm}$).^{10a}

It is worth pointing out that the (010) and $\bar{2}10$ crystallographic planes corresponding to these two reflections, in all the monoclinic δ -clathrates and in the δ form, are parallel to the closely packed ac layer of chains and to the loosely packed $c(b + a/2)$ layers of chains containing the guest locations, respectively. This is shown in Figure 4 for the δ form.

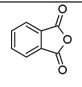
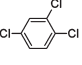
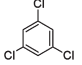
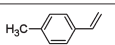
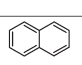
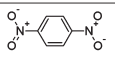
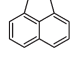
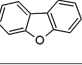
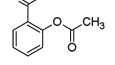
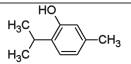
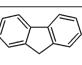
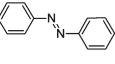
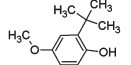
Table 1. Bragg Spacings (d_{010}) for s-PS δ -Clathrates with Different Guest Molecules^d

	Guest	Formula	Abbreviation	V_{mol} ($\text{nm}^3 \times 10^{-3}$) ^a	d_{010} (nm) ^b	Ref.
1	methylene chloride			58	1.08	7a
2	chloroform		CHCl ₃	73	1.13	7h
3	1,2-dichloroethane		DCE	76	1.06	7d
4	1,2-dichloropropane			94	1.08	15a
5	toluene		TOL	104	1.13	7b
6	nitrobenzene		NB	110	1.12	7g
7	4-methylphenol			111	1.13	15b
8	styrene			115	1.12	15c
9	<i>o</i> -dichlorobenzene		<i>o</i> DCB	117	1.14	7f
10	4-chlorotoluene			118	1.12	15d
11	indene			121	1.16	Our data
12	<i>m</i> -xylene			121	1.16	15e
13	4-nitroaniline		NA	122	1.08	7g
14	<i>p</i> -xylene		<i>p</i> XY	122	1.13	7b
15	<i>o</i> -xylene			124	1.12	15f
16	sPS δ form	—	δ	125 ^c	1.06	10a

^a Guest volumes has been determined by the Connolly method using a probe radius of 0.11 nm and a density dot of 0.1 nm^{-2} . ^b The reported Bragg distance corresponds to the position of the lowest-angle reflection of the diffraction pattern for clathrates whose crystal structure has not been solved or to the calculated d_{010} when the crystalline structure is known. ^c Volume of the empty cavity.^{7h,10b} ^d The molecular formula, volume and the abbreviations used in Figure 5 are also reported. Guests are listed by increasing molecular volume.

For some cocrystals (e.g., those from curve e to curve h in Figure 3A), we observe only one asymmetrical reflection, in the range $8.5\text{--}10.5^\circ$ and in which we can suppose the two reflections 010 e $\bar{2}10$ are merged. In these cases, the task to accurately determine the position of the 010 reflection; i.e., the distance between the *ac* layers (d_{010}), becomes difficult. However, as described in previous papers on the uniplanar orientations of s-PS,⁴ the intensity of the 010 reflection (both in X-ray diffraction patterns taken by having the X-ray beam parallel (EDGE) to the film surface or taken with an automatic powder diffractometer) is maximized for films exhibiting the $a_{\parallel}c_{\parallel}$ uniplanar orientation,^{4a,d} for which the *ac* layers (Figure 1) are preferentially parallel to the film plane.

This is shown, for instance, by the X-ray powder diffraction patterns, as obtained by an automatic diffractometer, of s-PS films exhibiting the same crystalline and cocrystalline phases of Figure 3A and degree of uniplanar $a_{\parallel}c_{\parallel}$ orientation close to 0.75 (Figure 3B). It is clearly apparent that the availability of films with uniplanar $a_{\parallel}c_{\parallel}$ orientation gives the opportunity to determine with a very good accuracy the d_{010} spacing of all s-PS cocrystalline phases, independent of the intensity of the (010) reflection.

	Guest	Formula	Abbreviation	V_{mol} ($\text{nm}^3 \times 10^{-3}$) ^a	d_{010} (nm) ^b	Ref.
17	phthalic anhydride			125	1.03	Our data
18	1,2,4-trichlorobenzene			128	1.12	Our data
19	1,3,5-trichlorobenzene		TCB	129	1.06	This paper
20	4-methylstyrene			131	1.16	Our data
21	naphthalene			134	1.15	5c
22	1,4-dinitrobenzene		DNB	134	1.02	This paper
23	acenaphthene		ACE	158	1.09	Our data
24	dibenzofuran		DBF	159	1.06	This paper
25	acetylsalicylic acid			163	1.03	Our data
26	thymol			164	1.04	Our data
27	fluorene			167	1.04	Our data
28	azobenzene			179	1.02	Our data
29	2-tert-butyl-4-methoxyphenol		BHA	191	1.02	This paper

For the cocrystals of Figure 3, as well as for many other s-PS cocrystalline phases with a representative set of guest molecules, the d_{010} spacing are collected in Table 1, together with the guest molecular volume (V_{mol} , as calculated on the basis of the van der Waals radii). For all cocrystalline phases of Table 1, the d_{010} spacing has been reported in Figure 5, versus the guest molecular volume.

Figure 5 clearly shows that beside several δ clathrate structures (square symbols), in which there is a significant increase of the spacing between the *ac* layers ($d_{010} > 1.1 \text{ nm}$) with respect to the empty δ phase ($d_{010} = 1.06 \text{ nm}$) as expected for the standard monoclinic structures,^{7b–f,h} a lot of other clathrate forms (round symbols) presents a spacing between the *ac* layers similar or even reduced ($1.08 > d_{010} > 1.02 \text{ nm}$) with respect to the empty δ phase, despite these last molecular guests are characterized by a molecular volume almost equal or greater than that of other guest molecules.

A simple hypothesis could be that, like the s-PS/NA cocrystal,^{7g} also s-PS cocrystals with TCB, DNB, DBF, BHA (and so on) could present similar triclinic structures with inclined planar guest molecules rather than the usual monoclinic structure with perpendicular planar guest molecules. In order to confirm this hypothesis, the crystal structure

determination of the s-PS cocrystals with DNB (presenting the lowest d_{010} value) and for DBF (presenting a definitely bigger volume with respect to NA and DNB) have been afforded.

s-PS/DNB Crystal Structure Determination. First of all, it is worth noticing that, at variance from other clathrate forms for which a monoclinic structure has been proposed, the equatorial intensity profiles read on the fiber X-ray diffraction

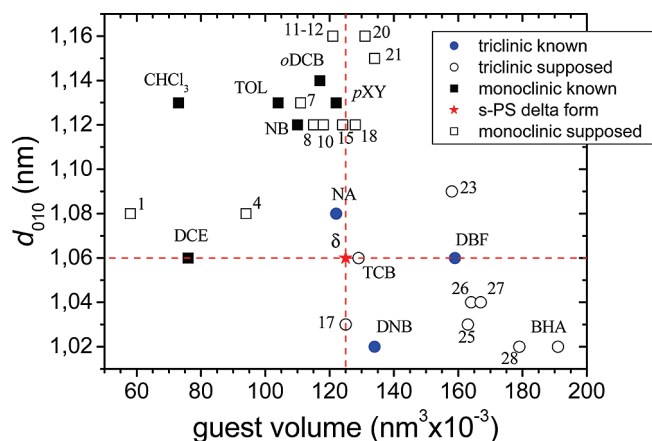


Figure 5. d_{010} distances for the s-PS δ -clathrates of Table 1 versus the guest molecular volume. Supposed or known monoclinic clathrates are indicated with empty or filled squares respectively, while supposed or known triclinic ones are indicated with empty or filled circles, respectively. The red star (whose position is highlighted by the two red dashed lines) indicates the d_{010} and volume of the cavities of the s-PS δ form.^{7h,10b} TOL = toluene; NB = nitrobenzene; pXY = *p*-xylene; oDCB = *o*-dichlorobenzene; NA = 4-nitroaniline; DCE = 1,2-dichloroethane; DBF = dibenzofuran; TCB = 1,3,5-trichlorobenzene; DNB = 1,4-dinitrobenzene; BHA = 2-*tert*-butyl-4-methoxyphenol. Numbers are reported according to Table 1.

patterns for this and of other clathrate forms supposed to be triclinic (see examples reported in Figure 3A) are characterized by only few and broad reflections suggesting the presence of some disorder.

Moreover as far the first layer line intensity profile (see Figure 3C), all these clathrate forms are characterized by a position of the most intense reflection in the region of 2θ 16–16.5°, as in the case of the s-PS/NA δ clathrate form and different from what was observed for the classical monoclinic clathrates for which the position of this reflection is in the region of 2θ 16.8–17.2°. The position of this reflection turned out to be strictly related to the value of the α angle of the unit cell.^{7g}

As for the s-PS/DNB δ clathrate, a X-ray fiber diffraction pattern of a uniaxially oriented film is reported in Figure 6 together with the intensity profiles read along the equatorial and first layer line. From the poorness of these data, in particular as far as the equatorial reflections, it can be understood that the determination of a unit cell accounting for the experimental data was far to be unique.

In order to determine a likely position of the reflections, owing to a conspicuous uniplanar orientation of the prepared films, we have also collected their through and edge diffraction patterns (whose intensity profiles, read along the equatorial and first layer line, are also reported in Figure 6). All the reflections identified in the fiber diffraction pattern are listed in Table 2.

Similar to the other δ clathrate forms of this polymer whose structure has been already reported in the literature,⁷ and supposing a simple extension of the triclinic model found in the case of the s-PS/NA δ clathrate,^{7g} also in these cases we indexed the first two equatorial reflections, located at $2\theta_{\text{CuK}\alpha} = 8.7^\circ$ and 9.7° , as 010 and $\bar{2}10$, respectively.

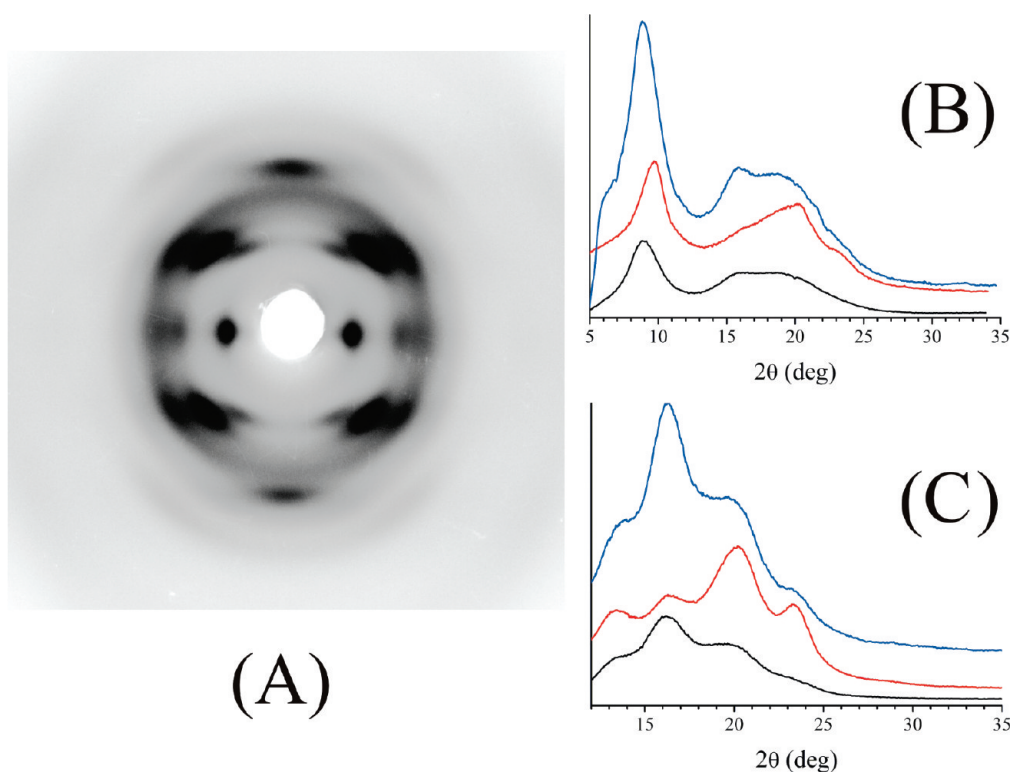


Figure 6. (A) X-ray fiber diffraction pattern of a uniaxially stretched film presenting the s-PS/DNB δ cocrystalline form. Fiber axis is vertical. Equatorial (B) and first layer line (C) intensity profile read on the diffraction pattern reported in part A (black line) and on a through (red line) and edge (blue line) diffraction patterns (not reported) of the same sample.

On the basis of the positions of the reflections listed in Table 2, a list of possible unit cells is reported in Table 3.

For all the proposed unit cells, we have then obtained minimum energy packing models imposing two guest per unit cell as proposed in the case of the δ -clathrate forms of s-PS with NA, under the $P\bar{1}$ symmetry. These models were all characterized by several nonbonded distances between C atoms certainly unacceptable (0.30–0.31 nm). This result was consistent with the fact that these models present too high densities, unexpected for cocrystalline phases with similar chemical composition (usually on the order of 1.10–1.15 g cm⁻³).⁷

Table 2. Diffraction Angles ($2\theta_{\text{obsd}}$) and Bragg Distances (d_{obsd}) of the Reflections Identified on the Layer Lines (l) of the X-ray Fiber Diffraction Pattern of the s-PS/DNB δ Clathrate Sample of Figure 6

l	$2\theta_{\text{obsd}}$ (deg)	d_{obsd} (nm)
0	8.7	1.02
0	9.7	0.91
0	15.8	0.56
0	18.8	0.47
0	20.1	0.44
1	13.4	0.66
1	16.2	0.55
1	19.6	0.45
1	23.0	0.39
2	24.5 ^a	0.36 ^a
2	28.5 ^a	0.31 ^a

^a Broad.

We have then hypothesized packing models characterized by only one guest molecule per unit cell (i.e., guest/monomer-unit molar ratio of 1/8). The minimum energy packing models obtained are quite similar to each other and all present acceptable nonbonded distances. Moreover they present a more reasonable density in respect to those previously proposed (see eighth column of Table 3). A representative packing model is given in Figure 7.

All the models corresponding to the unit cells of Table 3 give a reasonable agreement with the experimental data. Among these the model already presented in Figure 7 (corresponding to the unit cell no. 3 of Table 3) is that giving the best agreement with the experimental data (see Figure 8). Fractional coordinates for the model of Figure 7 and the complete list of calculated relative intensities are reported in Table 1 and 2 of Supporting Information.

s-PS/DBF Crystal Structure Determination. Analogous results have been obtained in the case of the crystal structure of the s-PS/DBF δ clathrate form for which the same procedure described in the case reported before has been followed. The X-ray fiber diffraction pattern of a uniaxially oriented film presenting the s-PS/DBF δ clathrate form is reported in Figure 9 together with the intensity profiles read along the equatorial and first layer line. All the reflections identified in the fiber diffraction pattern are listed in Table 4.

The packing model showing a best agreement with the experimental data is presented in Figure 10. The agreement with the experimental diffraction pattern is shown in Figure 11. Fractional coordinates for the model of Figure 10 and the

Table 3. Crystallographic Parameters of Some Possible Unit Cells Proposed for the s-PS/DNB δ Clathrate^a

	a (nm)	b (nm)	c (nm)	α (deg)	β (deg)	γ (deg)	ρ (guest/monomer-unit molar ratio of 1/4) (g/cm ³)	ρ (guest/monomer-unit molar ratio of 1/8) (g/cm ³)
1	1.88	1.27	0.79	102.5	90	124	1.29	1.10
2	1.85	1.29	0.79	102.5	90	125	1.28	1.12
3	1.83	1.30	0.79	102	90	126	1.32	1.14
4	1.79	1.32	0.79	102	90	127	1.35	1.16
5	1.79	1.33	0.79	101.5	90	128	1.35	1.17
6	1.78	1.35	0.79	101	90	129	1.36	1.17
7	1.78	1.37	0.79	101	90	130	1.36	1.17
8	1.79	1.38	0.79	100	90	132	1.38	1.18
9	1.80	1.43	0.79	100	90	134	1.37	1.17
10	1.82	1.49	0.79	100	90	135	1.32	1.13

^a The crystalline density in the hypothesis of a guest/monomer-unit molar ratio of 1/4 (i.e. two guests per unit cell) or of 1/8 (i.e., one guest per unit cell) has been reported too. The unit cells reported have been found by varying the γ angle in the range 124–135° by a step of 1° or 2° and by consequently optimizing the remaining unit cells parameters in such a way to index all the reflections listed in Table 2 and in particular indexing the first two equatorial reflection as 010 and $\bar{2}10$. c axis has been fixed to 0.79 nm as experimentally observed.

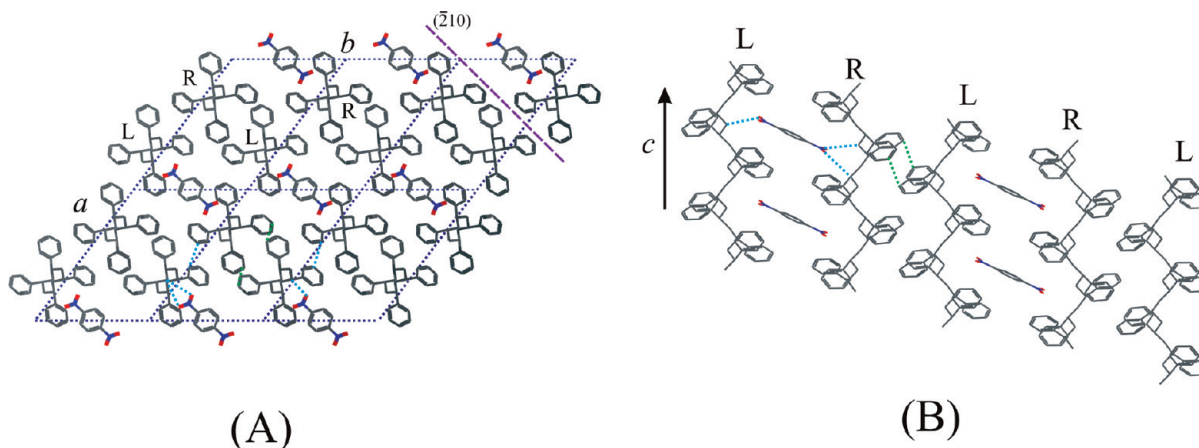


Figure 7. Packing model proposed for the crystal structure of s-PS/DNB δ cocrystalline form according to the space group $P\bar{1}$ in the unit cell no. 3 of Table 3. (A) View along the c axis. (B) View of a layer of enantiomorphous chains and of guest molecules along a direction perpendicular to the $(\bar{2}10)$ plane (whose trace is reported by a dashed line in part A). R = right-handed and L = left-handed helices. The shortest nonbonded distances between atoms are indicated (green for 0.33 nm and blue for 0.34 nm).

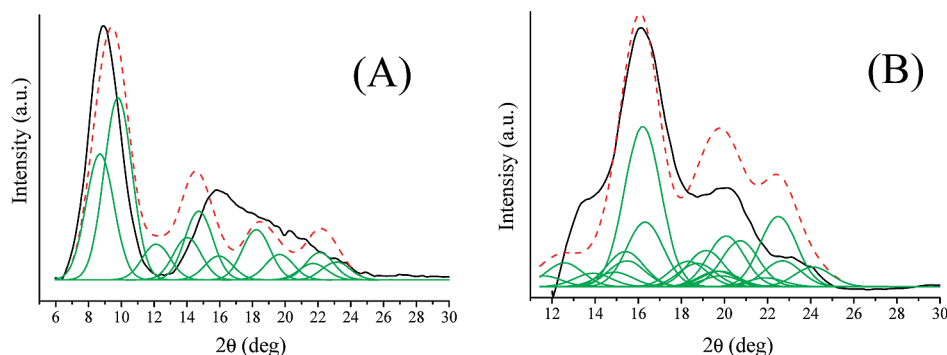


Figure 8. Equatorial (A) and first layer line (B) intensity profiles for the δ clathrate forms of s-PS with DNB: experimental (black continuous line) and calculated (red dotted line) according to the model reported in Figure 7. Green thin lines report as Gaussians the contributions to the calculated profile of each single significant reflection (intensity > 5% of the most intense one).

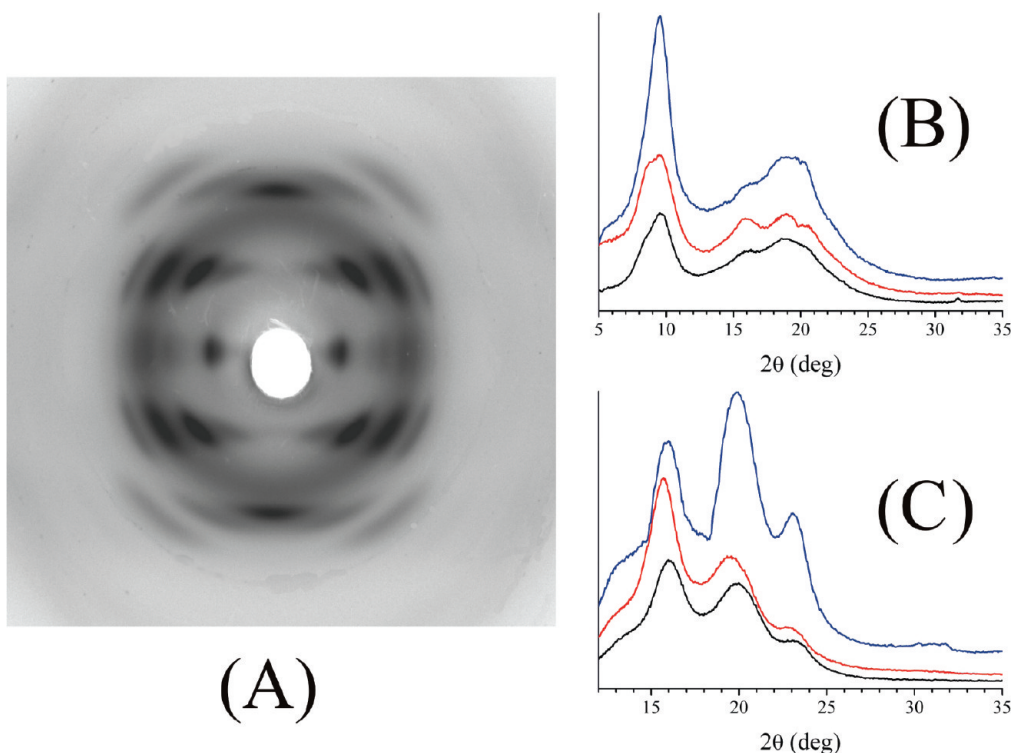


Figure 9. (A) X-ray fiber diffraction pattern of a uniaxially stretched film presenting the s-PS/DBF δ cocrystalline form. Fiber axis is vertical. Equatorial (B) and first layer line (C) intensity profile read on the diffraction pattern reported in part A (black line) and on a through (red line) and edge (blue line) diffraction patterns (not reported) of the same sample.

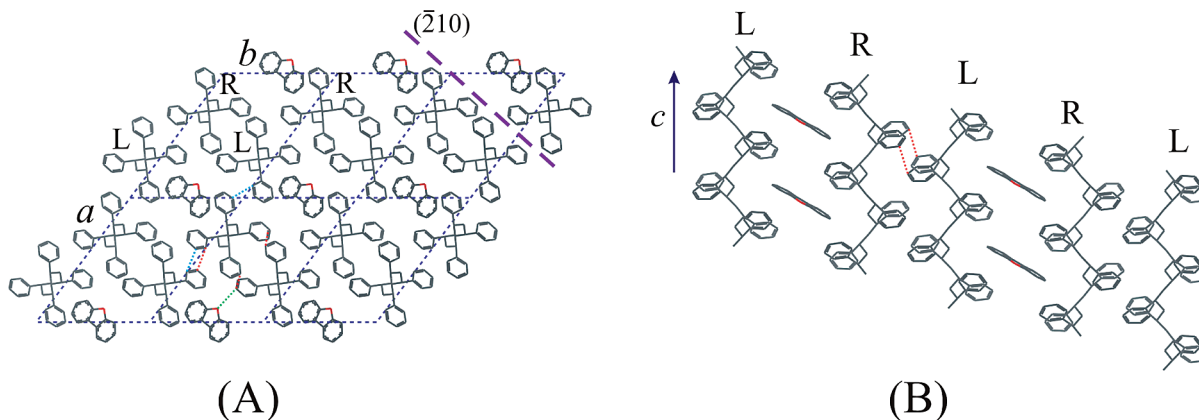


Figure 10. Packing model proposed for the crystal structure of s-PS/DBF δ clathrate according to the space group $P1$ in the unit cell $a = 1.82$ nm, $b = 1.36$ nm, $c = 0.79$ nm, $\alpha = 103^\circ$, $\beta = 90^\circ$, and $\gamma = 126^\circ$ ($d = 1.09$ g/cm³). (A) View along the c axis. (B) View of a layer of enantiomorphous chains and of guest molecules along a direction perpendicular to the $(\bar{2}10)$ plane (whose trace is reported by a dotted line in part A). R = right-handed and L = left-handed helices. The shortest nonbonded distances between atoms are indicated (green for 0.32 nm, red for 0.33 nm, and blue for 0.34 nm).

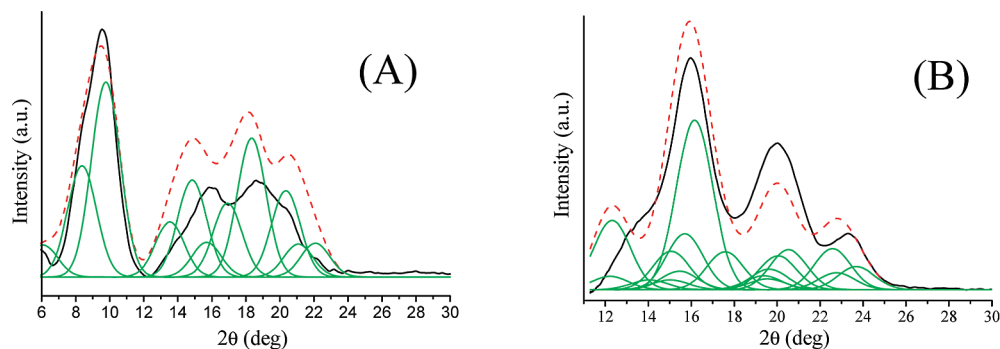


Figure 11. Equatorial (A) and first layer line (B) intensity profiles for the δ clathrate forms of s-PS with DBF: experimental (black continuous line) and calculated (red dotted line) according to the model reported in Figure 10. Green thin lines report as Gaussians the contributions to the calculated profile of each single significant reflection (intensity $> 5\%$ of the most intense one).

Table 4. Diffraction Angles ($2\theta_{\text{obsd}}$) and Bragg Distances (d_{obsd}) of the Reflections Identified on the Layer Lines (l) of the X-ray Fiber Diffraction Pattern of the s-PS/DBF δ Clathrate Sample of Figure 9

l	$2\theta_{\text{obsd}}$ (deg)	d_{obsd} (nm)
0	8.4	1.06
0	9.5	0.93
0	15.9	0.56
0	19.0	0.47
0	20.4	0.44
1	13.4	0.66
1	16.0	0.55
1	19.9	0.45
1	23.05	0.39
2	24.4 ^a	0.36 ^a
2	28.4 ^a	0.31 ^a

^a Broad.

complete list of calculated structure factors are reported in Table 3 and 4 of Supporting Information.

Comments on the Crystalline Structures. The crystalline structures of s-PS δ -clathrates with 1,4-dinitrobenzene and dibenzofuran described in the previous paragraphs, are characterized by triclinic unit cells and by guest molecular planes inclined with respect to the helical chain axes as already found in the case of the s-PS/NA δ clathrate form.^{7g} At the same time they present interesting new structural features. All the models are describable in terms of a sequence of layers of chains nearly parallel to the $\bar{2}10$ planes in which couples of close packed chains alternate to couples of chains delimiting regions in which guest molecules are hosted (see Figures 7B and 10B). In particular, in the case of DNB, within these layers distances between chain axis are near 1.24 nm (if guest are present) or 0.82 nm (for densely packed chains), whose mean value is consistent with the experimentally observed d_{010} (= 1.02 nm), while in the case of DBF, the distances between chain axis are in the range 1.32 nm (if guest are present) or 0.81 nm (for densely packed chains), whose mean value is consistent with the experimentally observed d_{010} (= 1.06 nm).

In this new organization of the δ -clathrate crystal structure, the close packing of the polymer chains along in the ac layers observed in all the δ -clathrate forms of this polymer described up to now (see Figure 1) is partially lost, since chain axes are not contained in this plane but are shifted by ± 0.11 nm in the case of s-PS/DNB (Figure 7A) and ± 0.13 nm in the case of s-PS/DBF (Figure 10A) clathrate forms.

Moreover, at variance with all the δ -clathrate forms of this polymer described up to now, the maximum guest/monomer-unit molar ratio is halved.

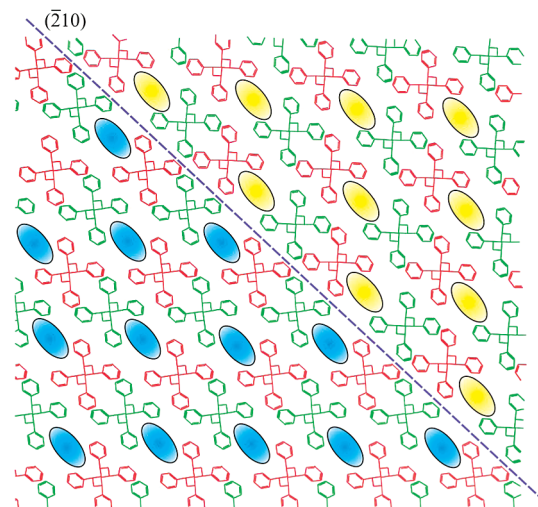


Figure 12. Schematic representation of a possible disorder present in the proposed structures for δ clathrates with DNB and DBF, showing two ordered local domains jointed along the $(\bar{2}10)$ plane (indicated with a dashed line). Enantiomorphic chains are reported in red (right handed) and green (left handed). Guest locations belonging to each of the two domains are reported in blue and yellow.

We think that the proposed crystal structure for these triclinic δ clathrates with bulky guest molecules is a limit ordered structure, being present only in small crystalline domains. The poorness of the experimental data, the larger broadness of the reflections in comparison with those for classical monoclinic structures (see Figure 3A) and the fact that no reflection is present on the equatorial layer line at 2θ higher than $20\text{--}21^\circ$ indicate that a high degree of disorder is present in the crystalline structure.

A possible disorder in the proposed structures is presented in Figure 12 in which two ordered local domains are jointed along the $(\bar{2}10)$ plane. According to our calculation the proposed junction between different domains is energetically feasible (less than 1 kcal/mol of unit cell) in respect to the minimum energy situation for a perfect crystal.

Other possible disorders can be due to faulted alternation of full and empty zones along the $(\bar{2}10)$ plane and to a not univocal position of the guest in the cavity.

Conclusions

The paper compares X-ray diffraction patterns of δ -clathrates of s-PS with a large number (28) of guests, having molecular volume in the range $0.058\text{--}0.195\text{ nm}^3$, mainly focusing on the distance between the ac layers of enantiomorphous polymer

helices (d_{010}). This distance has been precisely evaluated by effecting X-ray diffraction measurements on films exhibiting the a_{011} uniplanar orientation, i.e., the ac planes preferentially parallel to the film plane. The paper also reports the crystal structure determination of the δ -clathrates of s-PS with dinitrobenzene (DNB) and dibenzofuran (DBF).

The whole set of data of this paper, combined with the information already available in the literature, allows one to conclude that the δ -clathrates of s-PS can be divided into two different classes: monoclinic and triclinic.

In particular, monoclinic δ -clathrates are obtained with guests whose molecular volume is significantly lower to that one of the cavity of the δ nanoporous crystalline phase ($\approx 0.125 \text{ nm}^3$). In these monoclinic δ -clathrates the guest molecules are easily accommodated in the cavities of the δ phase, essentially only assisted by a possible increase of the distance between the ac layers of closely packed enantiomorphous polymer helices (d_{010}), thus maintaining a monoclinic unit cell and the $P2_1/a$ symmetry of the nanoporous δ form. Moreover, in the monoclinic δ -clathrates, the molecular planes of planar guest molecules assume an orientation perpendicular to the chain axes (Figure 2A). Because, in most cases, a single guest molecule is present in each cavity, the maximum molar ratio between guest molecules and styrenic units is 1/4.

On the other hand, triclinic δ -clathrates are obtained with guests whose molecular volume is significantly higher than that one of the cavity of the δ nanoporous crystalline phase ($\approx 0.125 \text{ nm}^3$).

Finally, guest molecules having a volume similar to the cavity volume of the δ phase present a more complex behavior. In these cases, in order to establish to which one of the two classes the clathrate belongs, it is important to determine the d_{010} spacing. In particular, for d_{010} spacing similar or lower than that the δ nanoporous crystalline phase clathrate structure are expected to be triclinic while for d_{010} spacing decidedly higher the structures are expected to be monoclinic.

For the triclinic δ -clathrate with 4-nitroaniline (NA) having a guest with a volume similar to the cavity volume of the δ phase, and showing only a minor increase of the d_{010} spacing, NA molecules are accommodated in all the isolated cavities of the δ phase, mainly by shifting the ac layers along the chain axis, thus leading to a triclinic (rather than monoclinic) unit-cell and to guest molecular planes inclined with respect to the helical chain axes (Figure 2B). Also in this case the maximum molar ratio between guest molecules and styrenic units is 1/4.

The triclinic δ -clathrates obtained with guests having molecular volume higher than the cavity volume of the δ phase, like DNB ($V_{\text{mol}} \approx 0.134 \text{ nm}^3$) and DBF ($V_{\text{mol}} \approx 0.159 \text{ nm}^3$), and a d_{010} spacing shorter or equal to that of the δ form, present interesting new structural features. In fact, these structures are still characterized by triclinic unit cells but can be described in terms of a sequence of layers of chains near parallel to the $\bar{2}10$ planes, in which couples of close packed chains are alternated with couples of chains delimiting the cavities where the guest molecule are hosted. In these triclinic δ -clathrates with bulky guests, the close packing of the polymer chains along in the ac layers is partially lost and one-half of the cavities initially present in the δ phase is lost while the other one-half increases its volume and becomes suitable to host bulky guest molecules (Figures 7 and 10). This of course halves the maximum guest/monomer-unit molar ratio that becomes 1/8. It is worth noting that δ -clathrates with most bulky guests (like those with molecular volume larger than 0.14 nm^3 , e.g., those corresponding to entries 23–29 in Table 1) are expected to exhibit analogous triclinic structures.

Finally, it is worth pointing out that the discovery of this new type of structural organization for the s-PS δ -clathrates discloses the possibility of obtaining cocrystalline structures with a large

number of bulky guests, hopefully with interesting new chemical and physical properties.

Acknowledgment. We thank Dr. Maria Maddalena Schiavone of University of Napoli and Prof. Vincenzo Venditto and Dr. Paola Rizzo of University of Salerno for useful discussions. Financial support of the “Ministero dell’Istruzione, dell’Università e della Ricerca” (PRIN2007), of “Regione Campania” (Legge 5) and of the Consortium INSTM (PRISMA01/2007 project) is gratefully acknowledged.

Supporting Information Available: Tables of the fractional coordinates of the proposed models and the complete calculated intensities. This material is available free of charge via the Internet at <http://pubs.acs.org>.

References and Notes

- (1) (a) Yokoyama, M.; Ishihara, H.; Iwamoto, R.; Tadokoro, H. *Macromolecules* **1969**, *2*, 589. (b) Point, J. J.; Coutelier, C. *J. Polym. Sci., Polym. Phys. Ed.* **1985**, *23*, 231. (c) De Rosa, C.; Petraccone, V.; Guerra, G.; Manfredi, C. *Polymer* **1996**, *37*, 5247. (d) Paternostre, L.; Damman, P.; Dosiè, M. *Macromolecules* **1999**, *32*, 153. (e) Matsumoto, A.; Odani, T.; Sada, K.; Miyata, M.; Tashiro, K. *Nature* **2000**, *405*, 328. (f) De Girolamo Del Mauro, A.; Loffredo, F.; Venditto, V.; Longo, P.; Guerra, G. *Macromolecules* **2003**, *36*, 7577. (g) Oshita, S.; Matsumoto, A. *Langmuir* **2006**, *22*, 1943. (h) Tarallo, O.; Esposito, G.; Passarelli, U.; Petraccone, V. *Macromolecules* **2007**, *40*, 5471.
- (2) Ishihara, N.; Seimiya, T.; Kuramoto, M.; Uoi, M. *Macromolecules* **1986**, *19*, 2464. (b) Zambelli, A.; Longo, P.; Pellicchia, C.; Grassi, A. *Macromolecules* **1987**, *20*, 2035. (c) Malanga, M. *Adv. Mater.* **2000**, *12*, 1869. (d) Schellenberg, J. *Prog. Polym. Sci.* **2009**, *34*, 688.
- (3) (a) Guerra, G.; Vitagliano, M. V.; De Rosa, C.; Petraccone, V.; Corradini, P. *Macromolecules* **1990**, *23*, 1539. (b) Chatani, Y.; Shimane, Y.; Inoue, Y.; Inagaki, T.; Ishioka, T.; Iijitsu, T.; Yukimori, T. *Polymer* **1992**, *33*, 488. (c) Gowd, E. B.; Tashiro, K.; Ramesh, C. *Prog. Polym. Sci.* **2009**, *34*, 280. (d) Milano, G.; Guerra, G. *Progr. Mater. Sci.* **2009**, *54*, 68. (e) Schellenberg, J. *Syndiotactic Polystyrene: synthesis, characterization, processing and applications*; Wiley: New York, 2010.
- (4) (a) Rizzo, P.; Lamberti, M.; Albunia, A. R.; Ruiz de Ballesteros, O.; Guerra, G. *Macromolecules* **2002**, *35*, 5854. (b) Rizzo, P.; Costabile, A.; Guerra, G. *Macromolecules* **2004**, *37*, 3071. (c) Rizzo, P.; Spatola, A.; De Girolamo Del Mauro, A.; Guerra, G. *Macromolecules* **2005**, *38*, 10089. (d) Albunia, A. R.; Rizzo, P.; Tarallo, O.; Petraccone, V.; Guerra, G. *Macromolecules* **2008**, *41*, 8632. (e) Albunia, A. R.; Rizzo, P.; Guerra, G. *Chem. Mater.* **2009**, *21*, 3370.
- (5) (a) Stegmaier, P.; De Girolamo Del Mauro, A.; Venditto, V.; Guerra, G. *Adv. Mater.* **2005**, *17*, 1166–1168. (b) Uda, Y.; Kaneko, F.; Tanigaki, N.; Kawaguchi, T. *Adv. Mater.* **2005**, *17*, 1846–1850. (c) Venditto, V.; Milano, G.; De Girolamo Del Mauro, A.; Guerra, G.; Mochizuki, J.; Itagaki, H. *Macromolecules* **2005**, *38*, 3696. (d) Kaneko, F.; Kajiwara, A.; Uda, Y.; Tanigaki, N. *Macromol. Rapid Commun.* **2006**, *27*, 1643. (e) D’Aniello, C.; Musto, P.; Venditto, V.; Guerra, G. *J. Mater. Chem.* **2007**, *17*, 531. (f) Daniel, C.; Galdi, N.; Montefusco, T.; Guerra, G. *Chem. Mater.* **2007**, *19*, 3302. (g) De Girolamo Del Mauro, A.; Carotenuto, M.; Venditto, V.; Petraccone, V.; Scoconi, M.; Guerra, G. *Chem. Mater.* **2007**, *19*, 6041. (h) Itagaki, H.; Sago, T.; Uematsu, M.; Yoshioka, G.; Correa, A.; Venditto, V.; Guerra, G. *Macromolecules* **2008**, *41*, 9156. (i) Daniel, C.; Albunia, A. R.; D’Aniello, C.; Rizzo, P.; Venditto, V.; Guerra, G. *J. Eur. Opt. Soc.-Rapid Publ.* **2009**, *4*, n09037. (j) Albunia, A. R.; D’Aniello, C.; Guerra, G.; Gatteschi, D.; Mannini, M.; Sorace, L. *Chem. Mater.* **2009**, *21*, 4750. (k) Rizzo, P.; Daniel, C.; Guerra, G. *Macromolecules* **2010**, *43*, 1882. (l) Albunia, A. R.; D’Aniello, C.; Guerra, G. *Cryst. Eng. Commun.* DOI: 10.1039/C0CE00128G.
- (6) (a) Petraccone, V.; Tarallo, O.; Venditto, V.; Guerra, G. *Macromolecules* **2005**, *38*, 6965. (b) Tarallo, O.; Petraccone, V.; Venditto, V.; Guerra, G. *Polymer* **2006**, *47*, 2402.
- (7) Immirzi, A.; de Candia, F.; Iannelli, P.; Zambelli, A.; Vittoria, V. *Makromol. Chem., Rapid Commun.* **1988**, *9*, 761. (b) Chatani, Y.; Shimane, Y.; Inagaki, T.; Iijitsu, T.; Yukimori, T.; Shikuma, H. *Polymer* **1993**, *34*, 1620. (c) Chatani, Y.; Inagaki, T.; Shimane, Y.; Shikuma, H. *Polymer* **1993**, *34*, 4841–4845. (d) De Rosa, C.; Rizzo, P.; Ruiz de Ballesteros, O.; Petraccone, V.; Guerra, G. *Polymer* **1999**, *40*, 2103. (e) Tarallo, O.; Petraccone, V. *Macromol. Chem. Phys.* **2004**,

- 205, 1351. (f) Tarallo, O.; Petraccone, V. *Macromol. Chem. Phys.* **2005**, *206*, 672–679. (g) Tarallo, O.; Petraccone, V.; Daniel, C.; Guerra, G. *Cryst. Eng. Commun.* **2009**, *11*, 2381. (h) Tarallo, O.; Schiavone, M. M.; Petraccone, V. *Eur. Polym. J.* **2010**, *46*, 456.
- (8) (a) Rizzo, P.; Daniel, C.; De Girolamo Del Mauro, A.; Guerra, G. *Chem. Mater.* **2007**, *19*, 3864. (b) Tarallo, O.; Schiavone, M. M.; Petraccone, V.; Daniel, C.; Rizzo, P.; Guerra, G. *Macromolecules* **2010**, *43*, 1455. (c) Daniel, C.; Montefusco, T.; Rizzo, P.; Musto, P.; Guerra, G. *Polymer* **2010**, *51*, 4599.
- (9) (a) Daniel, C.; Deluca, M. D.; Guenet, J. M.; Brulet, A.; Menelle, A. *Polymer* **1996**, *37*, 1273. (b) Rastogi, S.; Goossens, J. G. P.; Lemstra, P. J. *Macromolecules* **1998**, *31*, 2983. (c) van Hooij-Corstjens, C. S. J.; Magusin, P. C. M. M.; Rastogi, S.; Lemstra, P. J. *Macromolecules* **2002**, *35*, 6630. (d) Galdi, N.; Albunia, A. R.; Oliva, L.; Guerra, G. *Macromolecules* **2006**, *39*, 9171. (e) Malik, S.; Rochas, C.; Guenet, J. M. **2006**, *39*, 1000. (f) Buono, A. M.; Immediata, I.; Rizzo, P.; Guerra, G. *J. Am. Chem. Soc.* **2007**, *129*, 10992.
- (10) (a) De Rosa, C.; Guerra, G.; Petraccone, V.; Pirozzi, B. *Macromolecules* **1997**, *30*, 4147. (b) Milano, G.; Venditto, V.; Guerra, G.; Cavallo, L.; Ciambelli, P.; Sannino, D. *Chem. Mater.* **2001**, *13*, 1506. (c) Gowd, E. B.; Shibayama, N.; Tashiro, K. *Macromolecules* **2006**, *39*, 8412.
- (11) (a) Petraccone, V.; Ruiz de Ballesteros, O.; Tarallo, O.; Rizzo, P.; Guerra, G. *Chem. Mater.* **2008**, *20*, 3663. (b) Rizzo, P.; D'Aniello, C.; De Girolamo Del Mauro, A.; Guerra, G. *Macromolecules* **2007**, *40*, 9470. (c) Daniel, C.; Giudice, S.; Guerra, G. *Chem. Mater.* **2009**, *21*, 1028.
- (12) (a) Manfredi, C.; De Rosa, C.; Guerra, G.; Rapacciuolo, M.; Auriemma, F.; Corradini, P. *Macromol. Chem. Phys.* **1995**, *196*, 2795. (b) Larobina, D.; Sanguigno, L.; Venditto, V.; Guerra, G.; Mensitieri, G. *Polymer* **2004**, *45*, 429.
- (13) Sun, H. J. *Phys. Chem.* **1998**, *B 102*, 7338.
- (14) Corradini, P.; Napolitano, R.; Pirozzi, B. *Eur. Polym. J.* **1990**, *26*, 157.
- (15) (a) Musto, P.; Manzari, M.; Guerra, G. *Macromolecules* **2000**, *33*, 143. (b) Tsujita, Y.; Yoshimizu, H.; Okamoto, S. *J. Mol. Struct.* **2005**, *739*, 1873. (c) Reverchon, E.; Guerra, G.; Venditto, V. *J. Appl. Polym. Sci.* **1999**, *74*, 2077. (d) Manesh, K. P.O.; Sivakuram, M.; Yamamoto, Y.; Tsujita, Y.; Yoshimizu, H.; Okamoto, S. *J. Polym. Sci., Polym. Phys.* **2004**, *42*, 3439. (e) Yamamoto, Y.; Kishi, M.; amutharani, D.; Sivakumar, M.; Tsujita, Y.; Yoshimizu, H. *Polym. J.* **2003**, *35*, 465. (f) Loffredo, F.; Pranzo, A.; Venditto, V.; Longo, P. *Macromol. Chem. Phys.* **2003**, *204*, 859.